Green grinding-coassembly engineering toward intrinsically luminescent tetracene in cocrystals

Huang, Yinjuan; Gong, Qiuyu; Ge, Jing; Tang, Pengpeng; Yu, Fei; Xiao, Lian; Wang, Zongrui; Sun, Handong; Yu, Jing; Li, Dong-Sheng; Xiong, Qihua; Zhang, Qichun

2020

Huang, Y., Gong, Q., Ge, J., Tang, P., Yu, F., Xiao, L., Wang, Z., Sun, H., Yu, J., Li, D., Xiong, Q. & Zhang, Q. (2020). Green grinding-coassembly engineering toward intrinsically luminescent tetracene in cocrystals. ACS Nano, 14(11), 15962-15972. https://dx.doi.org/10.1021/acsnano.0c07416

https://hdl.handle.net/10356/154731

https://doi.org/10.1021/acsnano.0c07416

Green Grinding-Coassembly Engineering towards Intrinsically Luminescent Tetracene in Cocrystals

Yinjuan Huang,[1#] Qiuyu Gong,[1#] Jing Ge,[2] Pengpeng Tang,[3] Fei Yu,[1] Lian Xiao,[2] Zongrui Wang,[1] Handong Sun,[2] Jing Yu,[1] Dong-Sheng Li,[4] Qihua Xiong,[2]* Qichun Zhang[1,5]**

[1]School of Materials Science and Engineering, Nanyang Technological University, 639798, Singapore; [2]Division of Physics & Applied Physics, School of Physical and Mathematics Science, Nanyang Technological University, 639798, Singapore; [3]Nanjing Tsinghe Environmental Protection Technology Co., Ltd, 210001, Nanjing, Jiangsu Province, China; [4]College of Materials and Chemical Engineering, Key Laboratory of Inorganic Nonmetallic Crystalline and Energy Conversion Materials, China Three Gorges University, Yichang, Hubei 443002, P.R. China; [5]Department Materials Science and Engineering, City University of Hong Kong, Kowloon, Hong Kong SAR 999077, China.

Email address: qiczhang@cityu.edu.hk; qihua@ntu.edu.sg; lidongsheng1@126.com

ABSTRACT. Developing an effective and green method towards organic functional cocrystals based on the solubility-mismatched coformers is highly desirable and very important. Herein, we applied a green two-step liquid-assisted-grinding coassembly (LAGC) in fabricating tetracene-octafluoronaphthalene (TC-OFN) cocrystals from solubility-mismatched pairs of tetracene (TC, poorly soluble, 0.2 mg mL^{-1}) and octafluoronaphthalene (OFN, highly soluble, 0.2×10^4 mg mL^{-1}). Such cocrystals are extremely difficult to be prepared through the common solution-processing strategies. More importantly, this two-step LAGC process could allow us to efficiently prepare TC-OFN cocrystals in gram scale. The as-prepared cocrystals displayed the intrinsic green-emission of TC with much higher photoluminescence quantum yield (13.75%) comparing with the solid TC with the almost-quenched emission (0.41%, aggregation-caused quenching (ACQ)). The ultrafast spectra

study on these cocrystals verifies the successful barrier-function of OFN molecules in interrupting the well-known singlet-fission (SF) in TC solids. Furthermore, this method can allow us to easily fabricate fluorescent TC-OFN water inks, which can be employed to prepare luminescent paintings or highly emissive ultra-transparent/flexible films.

KEYWORDS: two-step, liquid-assisted-grinding coassembly, tetracene, intrinsic emission, solid state, cocrystal inks

Organic semiconducting materials not only are indispensable for fabricating advanced flexible and soft optoelectronic devices including field-effect transistors (FETs), light-emitting diodes (LEDs), and organic photovoltaics (OPVs), but also have wide applications in biological system.[1-6] Among all these materials, organic cocrystals have been demonstrated as multi-functional solids with tremendous research interests in numerous fields such as electronics, electroluminescent devices, photonics, and pharmaceutics.[7-18] However, there is a long-existing notorious issue in growing organic cocrystals,[19-21] namely, how to form cocrystals among solubility-mismatched components (at least one component has an extremely poor solubility). Although solution-processing methods (*i.e.* solvent evaporation, cooling, and anti-solvent addition) have been widely employed to grow organic cocrystals from all soluble starting molecules, the solubility-mismatched components (great difference in their solubility) usually result in single-phase crystals of the solubility-poor component while leaving the well-soluble one in solution. [19-23] Such an issue strongly encourages us to develop an effective cocrystallization method for the assembly of these solubility-mismatched coformer pairs into one crystal.

Grinding-cocrystallization, firstly studied in 1893, has been demonstrated to show numerous advantages over the solution-processing method including environmental friendliness, rapidness, and scalable yield.[24-25] Especially, the recently-developed liquid-assisted-grinding (LAG) has been proven to significantly increase the crystalline kinetics as well as control the polymorphs of the resultant cocrystals through appropriately applying

small quantities of solvents.[26] So far, this method is mainly applied in the system with the well-soluble coformers (*i.e.* drugs or organic non-functional small molecules).[24-26] Considering that the high solubility is not necessary in LAG,[24,27] it is reasonable for us to believe that LAG might overcome the above-mentioned solubility-mismatched issue between different conformers (especially solubility-mismatched organic functional coformers). However, such reports are rare.

Herein, we develop a modified LAG, namely green two-step liquid-assisted-grinding coassembly (LAGC) strategy, which has been adopted to successfully prepare TC-OFN (TC = tetracene and OFN = octafluoronaphthalene) cocrystals from solubility-mismatched pairs of TC (solubility, 0.2 mg mL^{-1}) and highly soluble OFN (solubility, 0.2×10^4 mg mL^{-1}). Such TC-OFN cocrystals are extremely difficult to be grown through the common solution-processing strategies (Figure 1, right-bottom). This two-step LAGC process is highly efficient (*i.e.* 80 mg products could be made in a total of 20 seconds), where the optimal TC/OFN ratio of 1:4 could totally transform TC to TC-OFN (Figure 1). More importantly, this method could allow us processing gram-scale compounds. Besides, the short grinding time could avoid the oxidation of unstable TC, which is generally observed in the solution-processing method without any protection. More importantly, solid TC molecules with serious aggregation-caused quenching (ACQ) could be strongly lighted up by OFN barriers. After cocrystalized with OFN, the solid TC with almost quenched emission (photoluminescence quantum yield, PLQY, 0.41%) emitted its intrinsic green-emission with much higher PLQY (13.75%) (Figure 1, right-top). Ultrafast spectra verified the mechanism that the periodic intercalation of weakly-fluorescent OFN barriers into the compacted molecular arrays of TC effectively interrupted the notorious SF process in TC solids. Furthermore, the highly luminescent TC-OFNs have been fabricated in water to form aqueous fluorescent water inks, which were employed to prepare luminescent paintings or highly emissive ultra-transparent/flexible films.

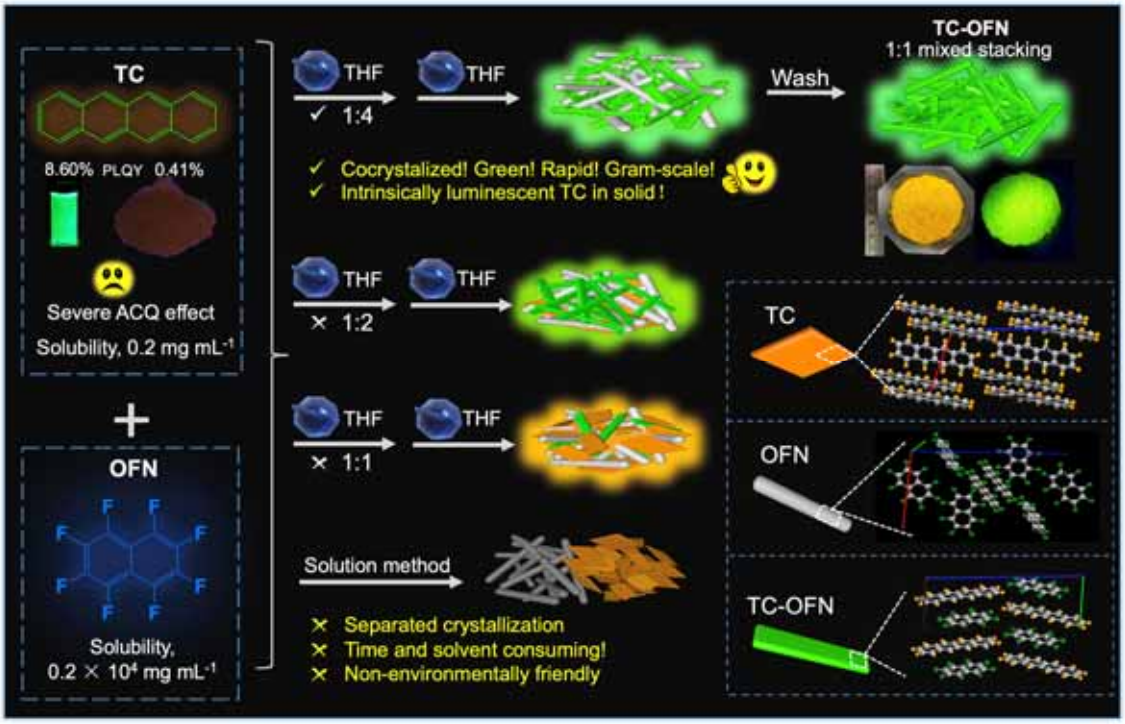

Figure 1. Illustrations of ACQ effect of TC and the preparation of target TC-OFN cocrystals. The PLQYs of the TC solution (THF as a solvent, concentration: 0.1 mg mL^{-1}) and solid TC as well as the solubilities (in THF) of TC and OFN are indicated (left). Comparison between the common solution-processing method and the current LAGC strategy is illustrated (right). Preparation of target TC-OFN cocrystals using TC/OFN ratio of 1:4 (right-top) compared with the cases of 1:2 (right-medium) and 1:1 (right-bottom), among which 1:4 ratio is the optimal condition towards pure TC-OFN. The photos of the resultant pure TC-OFN powders in gram-scale are indicated. The schematic morphologies of different crystals (TC crystals in orange, OFN crystals in gray, and TC-OFN cocrystals in green) as well as their molecular stacking modes are also indicated, and the CCDC numbers of TC crystal, OFN crystal, TC-OFN cocrystal are 1502159, 177726, and 1990854, respectively.

RESULTS AND DISCUSSION

Preparation. Before carrying out the two-step LAGC process, both solvent evaporation and cooling or anti-solvent addition methods to fabricate TC-OFN cocrystals have been tried, and none of them works due to their mismatched solubility, *i.e.* poor soluble TC and highly

soluble OFN (Figure S1, right-bottom of Figure 1). To solve this issue, a versatile LAGC methodology was applied because it can largely avoid either solvent effects and solubility issues in the solution-processed coassembly or the sublimation competition in the vapor-processed coassembly.[27] On the other hand, encouraged by our previous work,[18,28] OFN with a higher energy gap of *ca.* 3.78 eV could be used as a molecular barrier to prevent the intermolecular electron exchange and the interaction between TC molecules, which may further alleviate the severe ACQ of TC.

THF was chosen here due to its much better solubility for TC than any other common volatile solvents. Since the catalytic amount of THF and the grinding times have great impacts on the formation of cocrystals, it is necessary to optimize these conditions (Figure S2 and S3). In our research, we found that two-step grinding (10s each) with each entry of 0.04 mL THF can undoubtedly save both time and solvent amount, and this condition was chosen as the fixed parameters in further investigations. The detailed two-step LAGC processes are described as following: Total 80 mg of TC and OFN (mole ratio of TC/OFN = 1:1) were firstly ground for 10s in an agate mortar after rapidly adding 0.04 mL THF. Then, another batch of 0.04 mL THF was added to the above as-formed powder, and the resulted mixture was further ground for another 10 s to yield the luminescent product. Unfortunately, the mole ratio of 1:1 (TC to OFN) was not enough to transform all TC molecules into TC-OFN cocrystals, which motivated us to optimize this ratio. Therefore, other five different ratios (*i.e.* TC/OFN = 1:2, 1:3, 1:4, 1:6, and 1:8) together with pure TC and OFN have been tried and all results have been shown in Figure 2. These as-prepared samples were named as OFN, TC, 1:1, 1:2, 1:3, 1:4, 1:6 and 1:8 for the following discussion. During grinding, we found that with enough OFN, TC molecules could be completely transformed into cocrystals only in the second-step grinding although some cocrystals could be formed during the first-step process (Figure S4).

Optimization results. As shown in Figure 2a and b, pristine OFN (PLQY, 0.91%) and TC (PLQY, 0.41%) presented extremely weak blue- and orange-emission, respectively. However, when they were ground together with different ratios *via* LAGC process, green emission could be observed (Figure 2c-g, Figure S5, Table 1). The 1:1 powder presented inhomogeneous orange emission (PLQY: 1.31%) decorating with random green luminescence, while the 1:2 powder displayed yellow-green luminescence (PLQY: 5.42%). These results indicate that the transformation of TC to cocrystals is incomplete, which implies that largely excess OFN is very important to realize the full conversion of TC. In sharp contrast, with increasing the amount of OFN, the greatly enhanced green emission with much higher PLQY (13.31% for 1:3, 14.64% for 1:4, 12.83% for 1:6, 12.57% for 1:8) was observed, where 1:4 reached the maximum (Figure S6). These results suggest that the cocrystal strategy with OFN as molecular barriers could effectively reduce ACQ effect and realize the intrinsic emission of TC in solid state since TC in the diluted solution (PLQY:8.60%, Figure 1, left-top) emits green light.

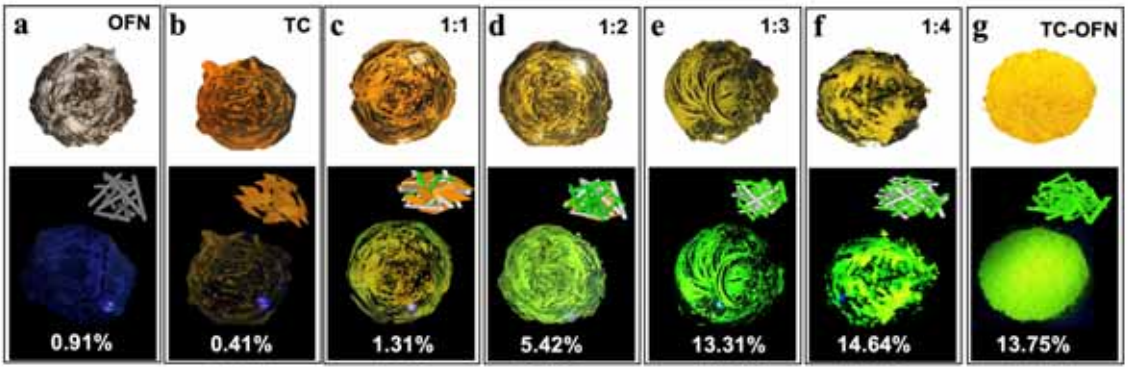

Figure 2. Optimization of TC/OFN ratios towards pure TC-OFN cocrystal. Photos of OFN (a), TC (b), 1:1 (c), 1:2 (d), 1:3 (e), 1:4 (f) and TC-OFN (g) in agate mortars under the irradiation of natural light (top) and UV lamp (bottom), respectively. The corresponding illustrated diagrams of phase composition and PLQYs are indicated.

Although 1:3, 1:6 or 1:8 powders could be purified to give pure cocrystals (TC-OFN) according to the different solubility between TC-OFN cocrystals and OFN molecules, the 1:4

sample was chosen for purification by considering its highest PLQY (Figure S7). The purification process was described in detail as following: 2 mL ethanol was added into 80 mg 1:4 powder, followed by sonication for 5 s. Afterwards, the remained solid was collected *via* vacuum filtration and dried in air for 1 h to yield pure TC-OFN cocrystals, whose structure was determined by single-crystal diffraction analysis (will be discussed in following section). More importantly, this method could allow us to prepare gram-scale pure TC-OFN cocrystals (PLQY, 13.75%) by using gram-scale TC and OFN as starting materials and proportionally increasing the amount of THF (Figure 2g). In order to further verify the universality of LAGC method in other cocrystal systems, coronene and perylene with good solubility were chosen. In this case, one equivalent molar OFN was enough to transform all the chromophore molecules into Cor/OFN or Per/OFN cocrystals (Figure S8-11). These results have been verified by PXRD patterns, which match well with the simulated files from their reported single-crystal structures (Figure S10 and S11).

Table 1. Key information of TC and the as-prepared samples *via* LAGC method

Sample name	TC	1:1	1:2	1:3	1:4	TC-OFN	TC solution [a]
PLQY [b]	0.41%	1.31%	5.42%	13.31%	14.64%	13.75%	8.60%
S_{abs} [c]	54 nm	49 nm	23 nm	23 nm	19 nm	23 nm	0
S_{em} [d]	33 nm	29 nm	20 nm	16 nm	16 nm	16 nm	0
Color-I [e]	Dark-orange	Orange	Yellow	Light-yellow	Light-yellow	Light-yellow	Light-yellow
Color-II [f]	Dark-orange	Orange	Yellow-green	Green	Green	Green	Green
Composition [g]	TC	TC, OFN, TC-OFN	TC, OFN, TC-OFN	OFN, TC-OFN	OFN, TC-OFN	TC-OFN	N/A

[a] TC solution in THF, 0.1 mg mL^{-1}. [b] Absolute quantum yield collected *via* integrating sphere method, average value of three tests. [c] Shifted wavelength of absorbance compared with that of TC solution. [d] Shifted wavelength of emission compared to that of TC solution. [e] Color of the samples under natural light. [f] Emission color of the samples under irradiation of UV lamp (365 nm). [g] Composition of crystal phase within the resultant powders.

The successful formation of TC-OFN cocrystals and the optimal mole ratio (TC/OFN) were further confirmed by UV-vis absorption and fluorescent spectra, Raman and Fourier Transform Infrared (FTIR) spectra, and Powder X-ray diffraction (PXRD) analyses. Figure 3a and b showed UV-vis absorption and photoluminescent (PL) spectra of all samples (solid OFN, solid TC, TC solution, 1:1, 1:2, 1:3, and 1:4). For clear comparison purpose, the absorption intensities in the region of 380 ~ 600 nm are enlarged eight times (Figure 3a). In this range, all as-prepared mixtures displayed blue-shifted absorption and emission compared with that of solid-state TC (Figure 3a and b, Figure S13 and S14). With the increasing amount of OFN, more blue shifts in UV absorption and emission were observed and these peaks became much closer to the intrinsic absorption of TC in dilute solution (Figure 3a and b, Figure S13 and S14). Especially for the 1:4 sample, its absorption and emission peaks are slightly red-shifted by 19 and 16 nm, respectively, compared with those of TC in solution. The detailed shifts have been summarized in Table 1. Moreover, the significantly improved photophysical properties were also directly verified by naked eyes based on the corresponding fluorescent photos (inset of Figure 3b). Pure TC in solid state displayed extremely weak orange emission, however, its emission could be blue-shifted with the color changes from orange-green to green when it was coassembled with the increasing amount of OFN. The above-mentioned blue-shifted absorptions should arise from blocking the formation of TC-TC dimers by electron-deficient molecular barriers of OFN that periodically intercalated between two adjacent TC molecules in the crystal *via* π-π and C-H…F interactions.[18,29] The blue-shifted emissions are ascribed to the screening of the π-interaction between two adjacent TC molecules by intercalated OFN molecule, which can significantly reduce the exciton-delocalization-induced PL red-shift.[18,29]

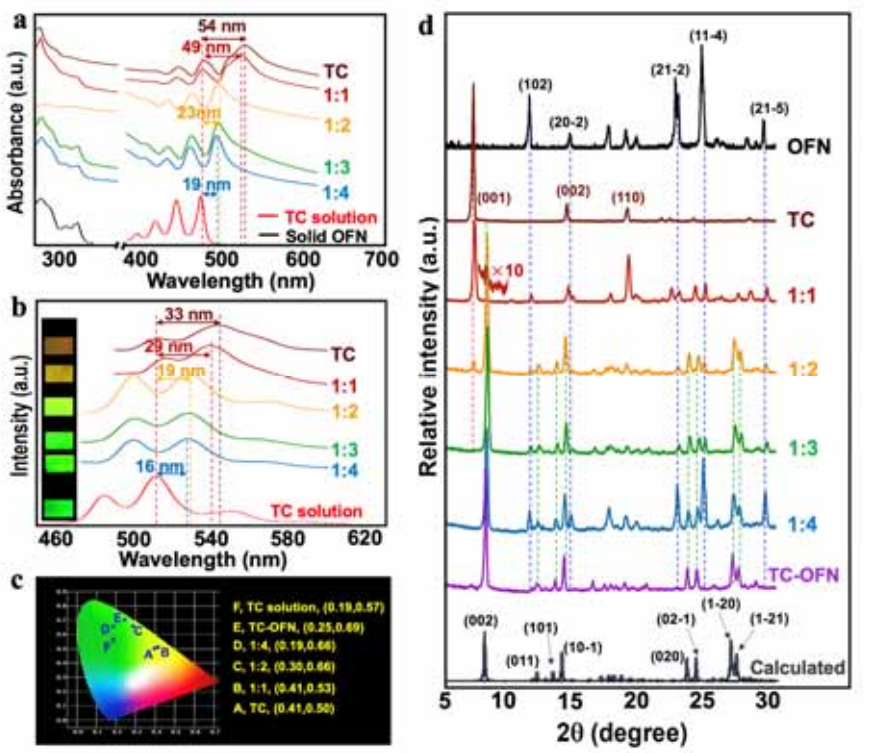

Figure 3. Supporting analysis of the optimization results toward TC-OFN. (a) Absorption spectra of solid-state OFN and TC, TC solution, as well as the un-purified 1:1, 1:2, 1:3, and 1:4 powders, respectively. The absorption intensities in the region of 380 to 600 nm are enlarged for eight times. (b) The corresponding PL spectra of (a), insets refer to the photographs of corresponding samples under irradiation of UV lamp (365 nm). (c) CIE chromaticity diagram of solid-state TC, TC solution and the resultant powders. (d) Experimental PXRD curves of OFN, TC and the resultant powders as well as the calculated PXRD curve of TC-OFN cocrystal. The blue, red and green dashed lines represent the peaks of OFN, TC and TC-OFN, respectively. Inset of 1:1, the peak of 8.2° is zoomed in for 10 times.

As we mentioned before, green fluorsecence is the intrinic emision of TC molecules in dilute solution. To more accurately compare the emission, the CIE chromaticity diagram of the as-prepared powders as well as TC in solution and solid-state has been provided in Figure 3c, where both the 1:4 powder and pure TC-OFN located at the same green area as that of TC solution, while the solid TC and 1:1 powder appearred in the yellow region (color offsetting

comes from the errors of naked eyes and CIE software), and the 1:2 sample located at the border between yellow and green regions. All these results clearly indicated that during grinding, electron-deficient OFN molecules can efficiently insert the crystal lattice of TC to completely separate TC molecules in space and disrupt the interaction and communication between neighboring TC molecules. Such arrangement would allow TC molecules to display their intrinsic photophysical properties in solid state.

The corresponding crystal phase composition within the resultant powders was listed in Table 1. As shown in Figure 3d, in contrast to pure OFN or TC, the PXRD patterns of all the as-prepared powders showed a new peak at 8.2°, which is associated with the characteristic phase of TC-OFN cocrystals, confirming the formation of new phase. However, the intensity of this peak in the 1:1 sample was extremely low, revealing that equimolar amount of OFN was far from enough to completely transform all TC molecules into cocrystals. When the amount of OFN was increased, this intensity increased greatly, accompanying with the gradual attenuation in the peak at 7.2° (belonging to pure TC phase, Figure 3d). This TC phase peak (7.2°) would eventually disappear when the ratio of TC/OFN reached 1:3 or above, indicating the complete transformation of TC into TC-OFN cocrystals.

Characterization and photophysical properties of TC-OFN cocrystal. The formation of TC-OFN cocrystals was further confirmed through *F*ourier *T*ransform *I*nfrared (FTIR) and Raman spectra. As shown in FTIR spectra (Figure S15), after grinding with TC, the original characteristic peaks of C-F bond in OFN migrated from 785 and 948 cm^{-1} [18,29] to 783 and 944 cm^{-1}, respectively, and the stretching signal of C-F bond in OFN shifted from 1203 cm^{-1} to 1196 cm^{-1}. Such migrations arised from the lengthened and weakened C-F bond attributed to the n→σ* donation in TC-OFN cocrystal.[29] At the same time, the chacteristic stretching peaks of Ar-H in TC moved from 3041 cm^{-1} and 2920 cm^{-1} to 3044 cm^{-1} and 2924 cm^{-1}, respectively, which were ascribed to the C-F···H interactions, suggesting the successful stacking between electron-deficient OFN and electron-rich TC.[29] These results clearly confirmed the formation

of TC-OFN phase (Figure S15). In Raman spectra (Figure S16), the original peaks of pure TC at 1159 cm^{-1} and 3076 cm^{-1} shifted to 1165 cm^{-1} and 3088 cm^{-1}, respectively, due to the decreased electron density of TC units in cocrystals,[30] further approving the formation of TC-OFN complex.

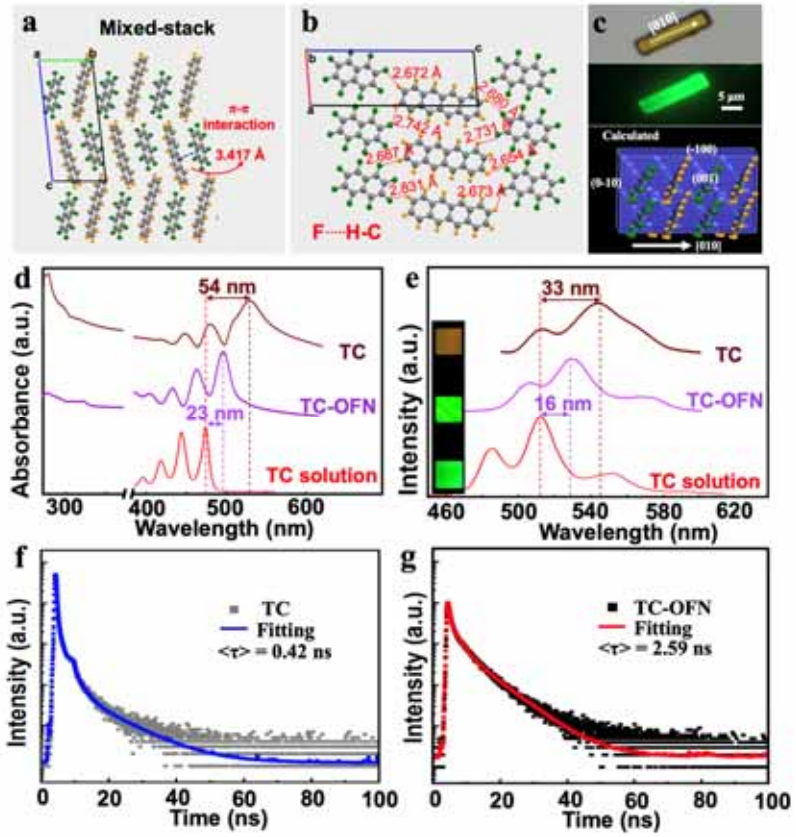

Figure 4. Structure characterization and photophysical properties of the target TC-OFN cocrystal. (a, b) Molecular mixed-stacking structure and intermolecular interactions, π-π interaction (a) and F…H bonds (b). (c) Bright-field (top) and fluorescence (medium) microscopy images of single crystalline TC-OFN and the calculated morphology (bottom) of TC-OFN based on the calculated energies. Absorption spectra (d) and PL spectra (e) of solid-state TC, TC solution and TC-OFN cocrystal, respectively. The absorption intensities in the region of 380 to 600 nm are enlarged for eight times. Time-resolved PL results of solid-state TC (f) and TC-OFN cocrystal (g), respectively. Concentration of TC solution in THF, 10^{-3} mg mL^{-1}.

The purification of 1:4 powder could provide TC-OFN micro cocrystals with high quality, however, their sizes were too small to be suitable for single-crystal diffraction analysis. Thus, the suitable single cocrystals for analysis were prepared by slow cooling of a large amount of molten OFN containing the dissolved TC. As shown in Figure 4a and b, Table S2 and Figure S17, 1:1 TC/OFN crystalizes in triclinic space (*P*-1) with the cell parameter of a = 6.548 (6) Å, b = 7.269 (6) Å, c = 21.261 (2) Å, α = 85.041 (3) deg, β = 84.946 (3) deg, γ = 89.943 (3) deg and V = 1004.34 (16) $Å^3$. All molecules adopt a mixed-stack mode, where TC and OFN alternately pack on each other *via* face-to-face pattern along the [010] or *b* direction, and the mean distance between adjacent TC and OFN (Figure 4a) is 3.417 Å, indicating the existence of π-π interactions between TC and OFN. Beside this force, numerous F···H-C bonds were formed between OFN and TC to generate pseudo 2D net in (010) plane (Figure 4b). Additionally, the [010] direction associated to the π–π stacking direction usually is the preferred growth direction of TC-OFN,[14,29] which resulted in the formation of one-dimensional well-defined cuboid assemblies rather than two-dimensional arrangement of TC molecules (Figure 4c, Figures S18-20).

Based on the above observations, a reasonable formation mechanism of TC-OFN is proposed here. Because of the extremely poor solubility of TC, the amount of OFN should be greatly excessive in order to completely transform all TC molecules into TC-OFN cocrystals. During the LAGC process, besides that the equimolar amount of OFN is consumed as the co-former of TC, the extra OFN acted as the solid solvent, which together with the catalytic THF promoted the intercalation of OFN molecules into TC phase. The function of THF can be regarded as a lubricant to create a medium to facilitate the molecular diffusion.[27,31] Moreover, during the two-step grinding, a small amount of THF was added in each step before grinding, which could greatly reduce the volatilization of THF without catalyzing the formation of cocrystals. Therefore, this two-step grinding towards complete cocrystallization can greatly save the solvent and time compared with the one-step grinding (detailed in Page S4). Note

that the catalytic rate increases with the increasing solubility of TC. Since TC has a better solubility in THF compared to the other common solvents, THF will be chosen as an auxiliary solvent in this research. The extra OFN in the case of 1:3 or above can be easily removed to produce pure TC-OFN micro cocrystals through washing with ethanol. The purity of the as-prepared TC-OFN phase was confirmed by PXRD patterns.

The photophysical properties of TC-OFN were demonstrated through UV-vis absorption and normal PL spectra (Figure 4d-g) as well as the time-resolved PL. For comparison, the photophysical properties of TC in dilute solution and solid state were also discussed here. Compared with those of TC dilute solution, the maximum absorption and emission of TC-OFN were slightly red-shifted by 23 and 16 nm, respectively (Figure 4d and e), while pure TC in solid state displayed large red-shifted absorption and emission spectra (54 and 33 nm, respectively). Moreover, TC-OFN powder emits green luminescence and has the highest PLQY (13.75%) among all three samples (0.41% for solid TC and 8.60% for TC in dilute solution). All results indicate that the tight stacking mode of TC molecules and the formation of TC-TC dimers in pure solid-state TC has been greatly destroyed by the periodically intercalated OFN molecular barriers, which agrees with the structural factors (*i.e.* mixed stacking, π-π and C-H…F interactions) of TC-OFN. Moreover, the difference in emission colors of these three samples (TC-OFN powder: green; TC solid: orange; TC in dilute solution: green) can be directly judged by naked eyes (Figure 4e, inset) and the CIE chromaticity diagram (Figure 3c), where pure TC-OFN exhibits the similar photophysical property to that (intrinsic) of TC in dilute solution. Furthermore, the time-resolved PL decays of pure TC and TC-OFN were conducted. As shown in Figure 4f and g, TC-OFN displays much longer lifetime of 2.59 ns than that (0.42 ns) of pristine TC in solid state (Figure S21). As reported in the literature,[32] TC in the dilute solution also has a much longer lifetime (4.2 ns) than that of pristine TC in solid state. All these results suggest that TC-OFN possesses the similar properties to that of single TC molecule.

Mechanisms for the intrinsic optical properties. As shown in Figure 5a, the intercalated OFN barriers shove two adjacent TC molecules and increased their distance to 6.834 Å, which is the main contribution to overcome ACQ effect appearing in pure TC in solid state. Generally, in pure TC crystal, the strong π…π stacking among the TC molecules would cause an efficient singlet-fission (SF) process (Figure 5b) [33-35] and possible ISC,[18,28] which may facilitate the formation of triplet state and finally give rise to the severe ACQ effect. However, benefiting from the periodic intercalation of weakly-fluorescent OFN barriers with a higher HOMO–LUMO gap of ~ 3.78 eV (calculated from the optical absorption in Figure S12a) into the compacted molecular arrays of TC (optical band gap, ~ 2.56 eV), the strong interactions and electronic coupling between TC molecules are greatly hindered (Figure 5a),[36] namely, the originally-existed SF and ISC processes in pure TC crystal will be cut off in TC-OFN system, leading to the absence of triplet states (Figure 5c, Figure S22).[28] Another possible reason might be that nonradiative relaxation pathways (rotational and vibrational) of excited states are greatly restrained[37] due to the rigidification and isolation of TC molecules in the TC-OFN cocrystals.[38]

Furthermore, the absence of triplet state during the excitation of TC-OFN cocrystals was verified by the transient absorption (TA) spectroscopy results (Figure 5d-g), where the complicated kinetics can be divided into the individual dynamics for singlet state and triplet state. As shown in Figure 5d, the signal at 500 nm should be assigned to singlet exciton (S_1) photoinduced absorption (PIA) due to the continuous decay feature. At longer time delays, the sharply absorption at 512 nm, which experienced the process of attenuation, generation and then attenuation, could be assigned to the triplet pair intermediate (TT) state resulted from the SF process.[33] To single out the TT generation, the kinetics at 512 and 493 nm were used, which were the locations of the maximum and the side of the TT absorption band, respectively. The kinetics were normalized to the peak of initial signal when only S1 was present, and then the difference between these two kinetics presented a background-free

kinetic, indicating the TT population evolution (Figure 5e).[33] However, the TT state kinetic in the TC-OFN cocrystals could not be observed (Figure 5f and g), suggesting a completely suppressed SF process, which is ascribed to that the screening effect of the TC-TC pairs by OFN barriers blocks the singlet-fission of TC-TC pairs. Unexpectedly, the triplet states populated by the possible ISC in the pristine TC as well as the ISC elimination in the TC-OFN cocrystal were not observed, which might be attributed to the dominant role of the SF process in the triplet formation of TC crystal. Generally speaking, the SF process could proceed in the systems of $E(S_1) > 2E(T_1)$,[33] indicating that a large singlet–triplet energy gap (ΔE_{ST}) is needed to achieve SF, *e.g.* the case of pristine TC system. Whereas, large ΔE_{ST} can undoubtedly suppress the singlet–triplet spin mixing (ISC),[39] leading to an insignificant ISC process.

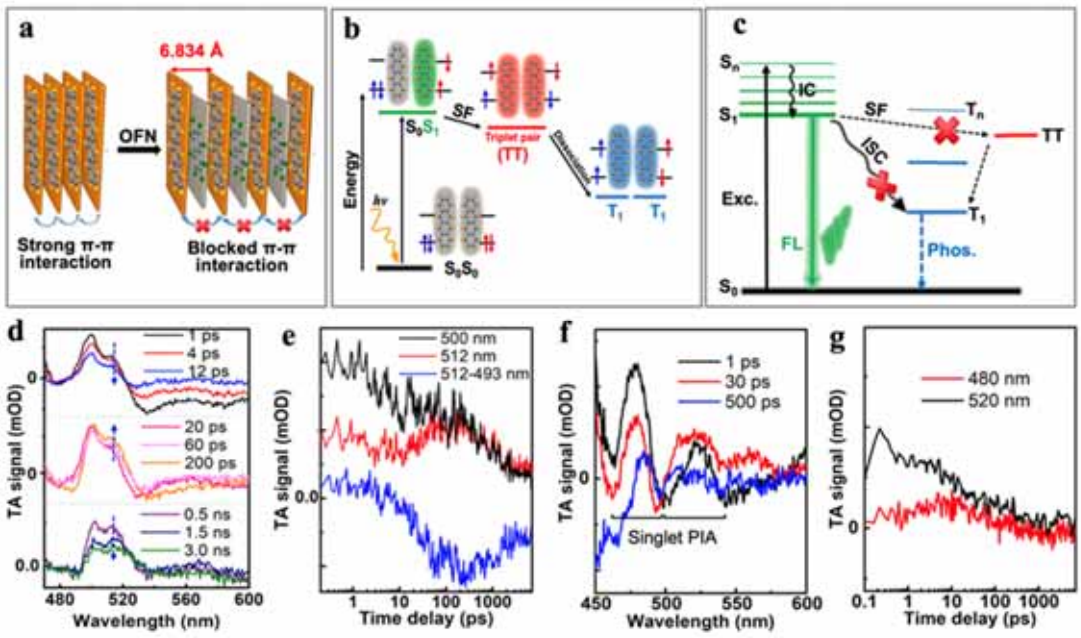

Figure 5. Mechanism investigations of the enhanced emission of TC-OFN. a) Schematic diagram of blocking π-π interaction between adjacent TC molecules. The enlarged distance between two TC planes (calculated by Diamond software) is indicated. b) Schematic diagram of SF process with pristine TC. c) Proposed emission mechanism based on Jablonski diagram of fluorescence of TC-OFN powder, where, S0, S1, T1 and TT refer to ground state, the lowest excited singlet state, lowest triplet state, and triplet pair, respectively. d) Ultrafast TA

spectra (from 1 ps to 3.0 ns) of TC powder. e) Corresponding kinetics (right, at 500 nm and 512 nm) and generation kinetic of the TT state (512-493 nm) of TC powder. The generation kinetic of the TT state was obtained by plotting the difference between the change in absorption at 512 nm (a TT absorption peak) and at 493 nm. The two kinetics were normalized at 0 ps and subtracted. f) TA spectra (from 1ps to 500 ps, left) of TC-OFN. g) Corresponding kinetics (right, at 480 nm and 520 nm) of TC-OFN. The absorptions in the regions of 463 ~ 495 nm and 500 ~ 543 nm are singlet PIA of TC-OFN cocrystal.

Applications. Benefiting from the readily preparation and gram-scale yield as well as highly emissive properties of the TC-OFN co-crystalline powder, this material would have great potential to be used as an advanced fluorescent ink. As shown in Figure 6a, the aqueous fluorescent TC-OFN inks could be easily prepared *via* grinding process by using poly(vinyl alcohol) (PVA)-containing water as the liquid medium. Note that the as-formed homogeneous ink displayed the similar optical properties compared with TC-OFN cocrystals (light-yellow color in daylight and bright green emission under UV lamp) (Figure 6a, Figure S23). For comparison, the corresponding TC and 1:1 inks were also prepared and utilized as the contrast. Subsequently, to demonstrate the possibility of the luminescent TC-OFN ink, the badge and iconic picture of NTU were firstly painted on a filter paper with three brush pens filled with the as-prepared luminescent inks and a commercially available pen (filled with red ink) (Figure 6a, b). Thanks to the significantly overcomed ACQ effect and the obviously different photophysical properties of three inks, the colorful badge and iconic picture of NTU were obtained under daylight after completely drying in air, where dark-orange TC, orange 1:1 and light-yellow TC-OFN inks could be easily distinguished (Figure 6b, left). Particularly, upon irradiation by a UV lamp (365 nm), much brighter green emission associated with the paintings of TC-OFN ink can be easily identified from these of the nearly invisible TC ink and weak orange-emissive 1:1 ink (Figure 6b, right) in the badge and ionic picture of NTU.

More impressively, the aqueous TC-OFN/PVA ink could also be used to fabricate highly luminescent films (TC-OFN@PVA) *via* a facile doctor-blade coating technique (Figure 6c). Notably, the resultant TC-OFN@PVA film possesses super-transparent and flexible features. Specifically, the golden badge with the name of "NANYANG TECHNOLOGICAL UNIVERSITY" could still be clearly seen, even the film was placed 25 cm far away from recording book. Additionally, such a transparent film can be freely bent or folded. Given the excellent flexibility and luminescent performance, a highly green-emissive windmill was fabricated based on the TC-OFN@PVA film, which shows great potential applications in the field of luminescent handicraft arts. All above achievements indicate the versatility of the aqueous fluorescent TC-OFN/PVA ink in both the painting/printing related fields and the flexible devices containing luminescent films.

Figure 6. Applications of TC-OFN as all-water dispersed fluorescent ink. a) Preparation of the all-water fluorescent inks. From left to right: TC powder, 1:1 powder, TC-OFN powder, PVA aqueous solution, TC ink, 1:1 ink, TC-OFN ink, schematic diagram of ink bottle and crayon. b) Hand-painted luminescent iconic-patterns of NTU on a filter paper under daylight

(left) and UV lamp (365 nm, right), respectively. c) Photographs of highly luminescent film (TC-OFN@PVA) and windmill based on TC-OFN using a black cover of recording book as back ground. From left to right: TC-OFN ink, photographs (under daylight) of TC-OFN@PVA film with D (the distance between film and recording book) of 1 cm, 25 cm by focusing on film and 25 cm by focusing on book, photographs (under 365 UV lamp) of rolled up film and windmill based on TC-OFN@PVA.

CONCLUSION

We here adopted a modified LAG, green two-step LAGC strategy, to successfully prepare non-reported TC-OFN cocrystal from the solubility-mismatched pairs of tetracene (poorly soluble) and octafluoronaphthalene (highly soluble), which is extremely difficult for the currently common solution-processing strategies. The two-step LAGC process under the optimal TC/OFN ratio of 1:4 presented the gram-scale yield and high efficiency. More importantly, after being cocrystalized with OFN, solid TC with almost quenched emission emitted its intrinsic green-emission with much higher PLQY. The periodic intercalation of weakly-fluorescent OFN barriers disrupts the intermolecular interactions and electronic coupling between the neighboring TC molecules, which further effectively blocks the originally-existing SF and possible ISC processes from singlet state to triplet state in pure TC crystals. Ultrafast spectra verified this mechanism. Besides, the as-prepared TC-OFN cocrystals can be readily dispersed into water to form aqueous inks. The unveiled emission endows the aqueous TC-OFN inks with highly luminescent feature, which could be further used to hand-paint luminescent iconic-patterns of NTU and fabricate highly green-emissive TC-OFN@PVA films with super-transparent and flexible features. Our achievements would undoubtedly provide important guidelines in the construction of new organic optoelectronic functional cocrystals based on the co-formers with mismatched solubility, which would also surely create more opportunities for “dark” TC or other planar polycyclic aromatic

compounds with ACQ effect in the applications of bioimaging, inkjet printing displays, and flexible optical devices.

METHODS

Characterization Methods. Powder X-ray diffraction (PXRD) patterns were collected on Bruker D8 diffractometer (German) equipped with Cu Kα radiation (λ = 1.5406 Å) under a scan rate of 0.02 deg s^{-1}. Single-crystal X-ray diffraction (SCXRD) data of TC-OFN cocrystals was collected on a Bruker SMART APEX-II CCD area detector equipped with a D8 goniometer. All the data were collected using the ω-scan method and 0.5 mm-Mono Cap-collimated and graphite-monochromated Mo-Kα radiation (λ = 0.71073 Å) was used. All the reduction and cell refinement were processed using the SAINT program of the APEX3 software. Area detector was corrected *via* multi-scan absorption by using the SADABS program. The TC-OFN structure was solved by the direct method and refined *via* the full-matrix least-squares method on F^2 (SHELX-2014). All non-H atoms were refined anisotropically. The hydrogen atoms were placed in the idealized positions and included as riding with U_{iso} (H) = 1.2 U_{eq} (C).

Ultraviolet-Visible (UV-vis) absorption data were obtained on UV-vis-NIR Cary 5000 spectrophotometer. The fluorescence data were collected on the Cary Eclipse Fluorescence Spectrophotometer. The solid samples for the absorption and emission spectra were fixed between two quartz plates before measurements. All the photoluminescence quantum yields (PLQYs) of the solid and liquid samples were determined by the quantum efficiency measurement system: QE-2100 (Qtsuka Electronics Co. Ltd., Japan) at 25 °C under air. Time resolved fluorescence measurements were conducted on the Fluoromax-4 Spectrofluorometer (France) at 25 °C under air. Raman spectra were obtained on the Nicolet iS50 FT-IR spectrometer equipped with an iS50 Raman module. Fourier transform infrared (FTIR) spectra were conducted on the Spectrum Frontier FTIR spectrometer (Perkin Elmer, Inc.) made in USA. Transmission electron microscopy (TEM)

were carried on the JEM-2100 (JEOL Ltd., Japan) with an accelerating voltage of 200 kV. Fluorescence microscopic images were captured on an Olympus IX73 Inverted Microscope System. The excitation wavelength is 488 nm with the exposure time of 60 ms when acquiring a photo. All the real photos of the samples were taken by an iPhone 8 Plus camera under the irradiation of hand-held UV lamp light (on/off).

Ultrafast transient absorption (TA) spectroscopy. The output pulse laser with 100 fs pulse width and 1 KHz repetition rate (800 nm) was generated from a commercial Ti: Sapphire regenerative amplifier (Spectra-Physics Spitfire) and split into two laser beams. One beam was sent to the optical parametric amplifier (Spectra-Physics TOPAS) to achieve pump pulses, where the wavelength center can be tuned from 290 to 2600 nm. Another beam went through a mechanical delay stage to pump a sapphire/CaF_2 crystal to form a light continuum that can serve as the probe pulse. The probe and pump pulses with a cross-polarization configuration were collinearly focused on the samples (beam size, 50 um and 100, respectively) *via* parabolic mirrors. In order to calculate a relative differential transmission, a mechanical chopper with a synchronized readout of a CMOS detector was applied for acquiring the probe spectra with and without pump-induced change. The pump laser with wavelength of 430 nm and (pump fluence)/(spot size) of ~350 $\mu J/cm^2$ were used for all measurements. The crystal dispersions (crystal concentration, 2 mg mL^{-1}, PVA concentration, 20 mg ml^{-1}) were used for the ultrafast TA measurement. The samples were placed in a quartz cuvette with the thickness of 3 mm during the measurements. All measurements were conducted in air.

Preparation of the crystal powders based on TC and OFN. TC represents the group of π-conjugated chromophores with an serious aggregation caused quench (ACQ) effect and poor solubility ($<$ 5 mg mL^{-1} in THF). Both solution- and vapor- methods have been ytried to fabricate TC-OFN cocrystals, however, none of them was successful, which indicates that it is extremely difficult to form cocrystals between the poorly-soluble π-conjugated chromophores and highly-soluble OFN molecules. Therefore, in this research, a clean and green liquid-

assisted grinding method was used to address such a tricky problem. Here, OFN was employed as the molecular barrier to overcome the ACQ Effect of TC and a convenient manual grinding was used during all the grinding experiments, wherein the grinding force was controlled to be roughly consistent.

Optimization of grinding times and solvent amount. In order to obtain the optimal grinding conditions, different grinding times (*e.g.* once, twice, three times and four times, respectively) and THF amount (*e.g.* 0.02, 0.04, 0.08 and 0.16 mL, respectively) were performed on 80 mg solid mixture of TC and OFN with a mole ratio of 1:4 (Figure S2). After 13.9 mg TC and 66.1 mg OFN were put into an agate mortar with an inner diameter of 6 cm, 0.02 ml THF was rapidly added in, and the resulted mixture was manually grinded for 10 s to form uniform powder. Then, another 0.02 ml THF was added and the resulted powder was grinded for another 10 s or more times. The real photos (with 365 nm UV light on and off) of the resulted samples after each grinding were recorded (Figure S2). Other THF amount conditions (*i.e.* 0.04, 0.08 and 0.16 mL) were also conducted according to the above procedures except for the THF amount. As shown in Figure S2 and S3, the entry of 0.04 mL THF can undoubtedly save both time (grinding for twice, spent 20 s) and solvent (totally need 0.08 mL). This as-obtained optimized condition (namely, grinding for twice, 0.08 mL (0.04 mL*2) THF per 80 mg sample) was chosen in further experiments.

Optimization of the ratios of TC to OFN. After TC and OFN with a certain mole ratio (*e.g.* 1:0, 1:1, 1:2, 1:3, 1:4, 1:6 and 1:8, respectively) and the constant total amount of 80 mg were put into an agate mortar with an inner diameter of 6 cm, 0.04 mL THF was rapidly added in and the resulted mixtures was grinded for 10 s to form uniform powder. Then, additional 0.04 mL THF was added and the resulted powder was grinded again for 10 s. Taking 1:4 as an example, the grinding procedure was provided in Figure S4. The resultant powders were collected and dried under air to give a yield of ~ 96%. The as-obtained seven

samples are named as TC, 1:1, 1:2, 1:3, 1:4, 1:6 and 1:8 powders, respectively. The corresponding colors for the two grinding stages are listed in Table S1.

Preparation of TC-OFN micro cocrystal. Given that the 1:4 sample presented the highest PLQY (Figure S6), it was chosen to be further purified to obtain the pure TC-OFN cocrystals. Ethanol was used to remove the excess OFN. Detailly, 2 mL ethanol was added into the above 1:4 powder (80 mg), followed by sonication for 5 s. Afterwards, the remained solid was collected *via* vacuum filtration and then dried in air for 1 h, yielding pure TC-OFN. More importantly, gram-scale samples can be easily achieved by the usage of a large amount of TC and OFN as well as the proportionally increased THF.

Preparation of bulk single TC-OFN cocrystal for SXRD test. We tried all the solution and vaper methods under various conditions, however, none of them was successful. Thus, the melted OFN was used as a solvent to dissolve TC for the cocrystal growth. Specifically, the mixture of 1 mg TC and 500 mg OFN was heated at 80 ºC for 5 min. After cooling the solution slowly to room temperature, the as-formed TC-OFN cocrystals were embedded in the OFN crystals, which could be separated before conducting the SXRD experiment.

Preparation of the samples for Fluorescence microscopy and TEM. For fluorescence microscope test, the freshly-prepared micro-crystal powder (0.1 mg) without any dry treatment was directly put on a glass slide and visualized through fluorescence microscope. For TEM visualization, the freshly-prepared micro-crystal powder (0.1 mg) without any dry treatment was directly dispersed in 1 mL PVA aqueous solution (10 mg mL^{-1}), followed by sonication for 5 min. Afterwards, TEM samples were prepared by dropping the above-prepared dispersion (5 μL) onto a carbon-coated copper grid and standing for 1 h, and then the excess liquid was removed using filter paper before further drying for 1h. No any staining treatment was performed.

Preparation of the luminescent aqueous ink and film. The luminescent aqueous inks were prepared *via* a solvent-casting method by using PVA aqueous solution as the liquid medium. Taking the TC-OFN ink as an example, the preparation procedure is as follows: after the PVA aqueous solution (0.05 g mL^{-1}) was prepared *via* dissolving 1 g PVA in 20 mL DI water at 80 ^{o}C for 2 h, 10 mg TC-OFN was dispersed into 1 mL above PVA aqueous solution, which was then ground with mortar and pestle for 20 min to form a homogeneous TC-OFN ink. The TC and 1:1 inks were prepared according to the same procedures. The TC-OFN based luminescent film (TC-OFN@PVA) was prepared by directly drop-casting 0.5 ml TC-OFN ink onto a dry and clean silicon wafer (about 60 cm^2) and being dried under vacuum at 60 °C overnight to remove the residual water. After that, the light-yellow film with strong luminescence was obtained after peeling it off from the wafer substrate. The film was then cut into 5 cm x 5 cm pieces before using.

Calculation of the theoretical morphology. The theoretical morphology of TC-OFN micro cocrystals was calculated using Materials Studio 6.0 software by considering the attachment energy theory. The predicted morphology and attachment energies calculations were obtained *via* the universal force field method with ultra-fine quality in the Morphology module of the Material Studio software.

ASSOCIATED CONTENT

Supporting Information.

The supporting Information is available free of charge via the Internet at http://pubs.acs.org. Preparation of Per/OFN and Cor/OFN cocrystal powders; Comparison between the solubilities of OFN and TC; Optimization of THF volume and grinding times; The curves of the Entry number *versus* the total time and THF volume; Results of the resulted 1:6 and 1:8 samples after grinding; The curve of the PLQYs *versus* the mole ratios of TC to OFN; The photos of 1:4 samples before and after purification; Conditions and results of grinding

experiments for each sample; Grinding results of Per/OFN; Grinding results of Cor/OFN; Experimental and calculated PXRD spectra of Per/OFN cocrystal; Experimental and calculated PXRD spectra of Cor/OFN cocrystal; UV-vis and PL spectra of OFN in solid and solution; UV-vis spectra of the solid 1:3, 1:4, 1:6 and 1:8 samples; PL emission spectra of the solid 1:3, 1:4, 1:6 and 1:8 samples; FTIR spectra of OFN, TC, 1:4 and TC-OFN powders; Raman spectra of TC, 1:1, 1:2, 1:4 and TC-OFN powders; Crystallographic data and structure refinement parameters of TC-OFN cocrystal; Unit cell of the molecular packing structure of TC-OFN; Calculated attachment energies of different crystal facets of TC-OFN cocrystal; Optical characterization of the as-prepared powders; TEM images of TC and TC-OFN cocrystal; Optical characterization of the as-prepared powders; K_i, T_i and τ values of TC, 1:1, 1:2, 1:4 and TC-OFN cocrystal; Time-resolved PL results of the un-purified powders. Time-resolved PL results of 1:1, 1:2, and 1:4 powders, respectively; Proposed schematic diagram of interactions between OFN and TC; Photos of the three inks, TC, 1:1 and TC-OFN, respectively, under 365 nm UV light.

AUTHOR INFORMATION

Author Contributions

[#]Yinjuan Huang and Qiuyu Gong contributed equally to this work.

Notes

The authors declare no competing financial interest

ACKNOWLEDGMENTS

Q.Z. acknowledges financial support from AcRF Tier 1 (RG 111/17, RG 2/17, RG 114/16, RG 8/16) and Tier 2 (MOE 2017-T2-1-021 and MOE 2018-T 2-1-070), Singapore. Q.Z. also acknowledges the support from starting funding of City University of Hong Kong (9380117), 111 Project (D20015), and State Key Laboratory of Supramolecular Structure and Materials, Jilin University (sklssm2020041).

REFERENCES

(1) Yang, Z.; Mao, Z.; Xie, Z.; Zhang, Y.; Liu, S.; Zhao, J.; Xu, J.; Chi, Z.; Aldred, M. P. Recent Advances in Organic Thermally Activated Delayed Fluorescence Materials. *Chem. Soc. Rev.* **2017**, *46*, 915-1016.

(2) Nielsen, C. B.; Holliday, S.; Chen, H.-Y.; Cryer, S. J.; McCulloch, I. Non-Fullerene Electron Acceptors for Use in Organic Solar Cells. *Acc. Chem. Res.* **2015**, *48*, 2803-2812.

(3) Hill, M. T.; Gather, M. C. Advances in Small Lasers. *Nat. Photonics* **2014**, *8*, 908–918.

(4) Tang, W.; Yang, Z.; Wang, S.; Wang, Z.; Song, J.; Yu, G.; Fan, W.; Dai, Y.; Wang, J.; Shan, L., Niu, G., Fan, Q., Chen, X. Organic Semiconducting Photoacoustic Nanodroplets for Laser-Activatable Ultrasound Imaging and Combinational Cancer Therapy. *ACS Nano* **2018**, *12*, 2610-2622.

(5) Yin, C.; Wen, G.; Liu, C.; Yang, B.; Lin, S.; Huang, J.; Zhao, P.; Wong, S.H.D.; Zhang, K.; Chen, X., Li, G., Jiang, X., Huang, J., Pu, K., Wang, L., Bian, L. Organic Semiconducting Polymer Nanoparticles for Photoacoustic Labeling and Tracking of Stem Cells in the Second Near-Infrared Window. *ACS Nano* **2018**, *12*, 12201-12211.

(6) Duan, H.; Lyu, P.; Liu, J.; Zhao, Y.; Xu, Y. Semiconducting Crystalline Two-Dimensional Polyimide Nanosheets with Superior Sodium Storage Properties. *ACS Nano* **2019**, *13*, 2473-2480.

(7) Ji, W.; Xue, B.; Bera, S.; Guerin, S.; Liu, Y.; Yuan, H.; Li, Q.; Yuan, C.; Shimon, L.J.W.; Ma, Q., Kiely, E., Tofail, S. A. M., Si, M., Yan, X., Cao, Y., Wang, W., Yang, R., Thompson, D., Li, J., Gazit, E. Tunable Mechanical and Optoelectronic Properties of Organic Cocrystals by Unexpected Stacking Transformation from H- to J- and X-Aggregation. *ACS Nano* **2020**, *14*, 10704-10715.

(8) Zhu, W.; Zheng, R.; Zhen, Y.; Yu, Z.; Dong, H.; Fu, H.; Shi, Q.; Hu, W. Rational Design of Charge-Transfer Interactions in Halogenbonded Co-Crystals toward Versatile Solid-State Optoelectronics. *J. Am. Chem. Soc.* **2015**, *137*, 11038–11046.

(9) Lei, Y. L; Liao, L. S; Lee, S. T. Selective Growth of Dual-Color-Emitting Heterogeneous Microdumbbells Composed of Organic Charge-Transfer Complexes. *J. Am. Chem. Soc.* **2013**, *135*, 3744 – 3747.

(10) Ferraris, J.; Walatka, V.; Perlstei, J. H.; Cowan, D. O. Electron Transfer in a New Highly Conducting Donor-Acceptor Complex. *J. Am. Chem. Soc.* **1973**, *95*, 948 – 949.

(11) Kang, S. J.; Ahn, S.; Kim, J. B.; Schenck, C.; Hiszpanski, A. M.; Oh, S; Schiros, T.; Loo, Y.-L.; Nuckolls, C. Using Self-Organization to Control Morphology in Molecular Photovoltaics. *J. Am. Chem. Soc.* **2013**, *135*, 2207 – 2712.

(12) Xiao, J.; Yin, Z.; Li, H.; Zhang, Q.; Boey, F.; Zhang, H.; Zhang, Q. Postchemistry of Organic Particles: When TTF Microparticles Meet TCNQ Microstructures in Aqueous Solution. *J. Am. Chem. Soc.* **2010**, *132*, 6926 – 6928.

(13) Qin, Y.; Zhang, J.; Zheng, X.; Geng, H.; Zhao, G.; Xu, W.; Hu, W.; Shuai, Z.; Zhu, D. Charge-Transfer Complex Crystal Based on Extended-π-Conjugated Acceptor and Sulfur-Bridged Annulene: Charge-Transfer Interaction and Remarkable High Ambipolar Transport Characteristics. *Adv. Mater.* **2014**, *26*, 4093 – 4099.

(14) Lei, Y. L.; Jin, Y.; Zhou, D. Y.; Gu, W.; Shi, X. B.; Liao, L. S.; Lee, S. T. White-Light Emitting Microtubes of Mixed Organic Charge-Transfer Complexes. *Adv. Mater.* **2012**, *24*, 5345 – 5351.

(15) Tayi, A. S.; Shveyd, A. K.; Sue, A. C. H.; Szarko, J. M.; Rolczynski, B. S.; Cao, D.; Kennedy, T. J.; Sarjeant, A. A.; Stern, C. L.; Paxton, W. F., Wu, W., Dey, S. K., Fahrenbach, A. C., Guest, J. R., Mohseni, H.,Chen, L. X., Wang, K. L., Stoddart, J. F., Stupp, S. I. Room-Temperature Ferroelectricity in Supramolecular Networks of Charge-Transfer Complexes. *Nature* **2012**, *488*, 485 – 489.

(16) Tang, Y. Z.; Yu, Y. M.; Xiong, J. B.; Tan, Y. H.; Wen, H. R. Unusual High-Temperature Reversible Phase-Transition Behavior, Structures, and Dielectric–Ferroelectric Properties of Two New Crown Ether Clathrates. *J. Am. Chem. Soc.* **2015**, *137*, 13345 – 13351.

(17) Liu, G.; Liu, J.; Ye, X.; Nie, L.; Gu, P.; Tao, X.; Zhang, Q. Self-Healing Behavior in a Thermo-Mechanically Responsive Cocrystal during a Reversible Phase Transition. *Angew. Chem. Int. Ed.* **2017**, *56*, 198 – 202.

(18) Huang, Y.; Xing, J.; Gong, Q.; Chen, L.-C.; Liu, G.; Yao, C.; Wang, Z.; Zhang, H.-L.; Chen, Z.; Zhang, Q. Reducing Aggregation Caused Quenching Effect through Co-Assembly of PAH Chromophores and Molecular Barriers. *Nat. Commun.* **2019**, *10*, 169.

(19) Huang, Y.; Wang, Z.; Chen, Z.; Zhang, Q. Organic Cocrystals: Beyond Electrical Conductivities and Field-Effect Transistors (FETs). *Angew. Chem. Int. Ed.* **2019**, *58*, 9696 – 9711.

(20) Li, R.; Hu, W.; Liu, Y.; Zhu, D. Micro-and Nanocrystals of Organic Semiconductors. *Acc. Chem. Res.* **2010**, *43*, 529−540.

(21) Wang, Y.; Zhu, W.; Dong, H.; Zhang, X.; Li, R.; Hu, W. Organic Cocrystals: New Strategy for Molecular Collaborative Innovation. *Top Curr. Chem.* **2016**, *83*, 1-34.

(22) Friščić , T.; Trask, A. V.; Jones, W.; Motherwell, W. D. S. Screening for Inclusion Compounds and Systematic Construction of Three-Component Solids by Liquid-Assisted Grinding. *Angew. Chem. Int. Ed.* **2006**, *45*, 7546–7550.

(23) Lien Nguyen, K.; Friščić , T.; Day, G. M.; Gladden, L. F.; Jones, W. Terahertz Time-Domain Spectroscopy and the Quantitative Monitoring of Mechanochemical Cocrystal Formation. *Nat. Mater.* **2007**, *6*, 206–209.

(24) Braga, D.; Maini, L.; Grepioni, F. Mechanochemical Preparation of Co-Crystals. *Chem. Soc. Rev.* **2013**, *42*, 7638-7648.

(25) Trask, A. V.; Jones, W. Crystal Engineering of Organic Cocrystals by the Solid-State Grinding Approach. *Top Curr. Chem.* **2005**, *254*, 41– 70.

(26) Shan, N.; Toda, F.; Jones, W. Mechanochemistry and Co-Crystal Formation: Effect of Solvent on Reaction Kinetics. *Chem. Commun.* **2002**, *20*, 2372–2373.

(27) Friščić, T.; Jones, W. Recent Advances in Understanding the Mechanism of Cocrystal Formation *via* Grinding. *Cryst. Growth Des.* **2009**, *9*, 1621–1637.

(28) Ye, H.; Liu, G.; Liu, S.; Casanova, D.; Ye, X.; Tao, X.; Zhang, Q.; Xiong, Q. Molecular-Barrier-Enhanced Aromatic Fluorophores in Cocrystals with Unity Quantum Efficiency. *Angew. Chem. Int. Ed.* **2018,** *57*, 1928-1932.

(29) Hanson, G. R.; Jensen, P.; McMurtrie, J.; Rintoul, L.; Micallef, A. S. Halogen Bonding between An Isoindoline Nitroxide and 1,4-Diiodotetrafluorobenzene: New Tools and Tectons for Self-Assembling Organic Spin Systems. *Chem. - Eur. J.* **2009,** *15*, 4156–4164.

(30) Kenji, Y.; Shiro, M. A Study of Electronic Structure of 1,2,4,5-Tetracyanobenzene Anion Radical by Resonance Raman Effect. *Chem. Soc. Jpn.* **1980,** *53*, 1949–1955.

(31) Braga, D.; Giaffreda, S. L.; Rubini, K.; Grepioni, F.; Chierotti, M. R.; Gobetto, R. Making Crystals from Crystals: Three Solvent-Free Routes to the Hydrogen Bonded Co-crystal between 1,1′-Di-Pyridyl-Ferrocene and Anthranilic Acid. *Cryst. Eng. Comm.* **2007**, *9*, 39–45.

(32) Burdett, J. J.; Müller, A. M.; Gosztola, D.; Bardeen, C. J. Excited State Dynamics in Solid and Monomeric Tetracene: The Roles of Superradiance and Exciton Fission. *J. Chem. Phy.* **2010**, *133*, 144506.

(33) Stern, H. L.; Cheminal, A.; Yost, S. R.; Broch, K.; Bayliss, S. L.; Chen, K.; Tabachnyk, M.; Thorley, K.; Greenham, N.; Hodgkiss, J. M., Anthony, J., Head-Gordon, M., Musser, A. J., Rao, A., Friend, R. H. Vibronically Coherent Ultrafast Triplet-Pair Formation and Subsequent Thermally Activated Dissociation Control Eefficient Endothermic Singlet Fission. *Nat. Chem.*, **2017**, *9*, 1205 – 1212.

(34) Dover, C. B.; Gallaher, J. K.; Frazer, L.; Tapping, P.; Petty, C. A; Crossley, J. M. J.; Anthony, J. E.; Kee, T. W.; Schmidt, T. W. Endothermic Singlet Fission is Hindered by Excimer Formation. *Nat. Chem.* **2018**, *10*, 305 – 310.

(35) Zeiser, C.; Moretti, L.; Lepple, D.; Cerullo, G.; Maiuri M.; Broch. K. Singlet Heterofission in Tetracene-Pentacene Thin-Film Blends. *Angew. Chem. Int. Ed.* **2020**, https://doi.org/10.1002/anie.202007412.

(36) Giacobbe, E. M.; Mi, Q.; Colvin, M. T.; Cohen, B.; Ramanan, C.; Scott, A. M.; Yeganeh, S.; Marks, T. J.; Ratner, M. A.; Wasielewski, M. R. Ultrafast Intersystem Crossing and Spin Dynamics of Photoexcited Perylene-3,4:9,10-bis(dicarboximide) Covalently Linked to a Nitroxide Radical at Fixed Distances. *J. Am. Chem. Soc.* **2009,** *131*, 3700–3712.

(37) Liu, Y.; Zeng, Q.; Zou, B.; Liu, Y.; Xu, B.; Tian, W. Piezochromic Luminescence of Donor–Acceptor Cocrystals: Distinct Responses to Anisotropic Grinding and Isotropic Compression. *Angew. Chem. Int. Ed.* **2018**, *57*, 15670 – 15674.

(38) Sun, Y.; Lei, Y.; Liao, L.; Hu, W. Competition between Arene–Perfluoroarene and Charge-Transfer Interactions in Organic Light-Harvesting Systems. *Angew. Chem. Int. Ed.* **2017**, *56*, 10352 –10356.

(39) Sun, L.; Hua, W.; Liu, Y.; Tian, G.; Chen, M.; Yang, F.; Wang, S.; Zhang, X.; Luo, Y.; Hu, W. Thermally Activated Delayed Fluorescence in an Organic Cocrystal: Narrowing the Singlet–Triplet Energy Gap *via* Charge Transfer. *Angew. Chem. Int. Ed.* **2019**, *58*, 11311-11316.

For Table of Contents Only